

Ordinary Objects come to the aid of Investigation of Gas Explosion Incidents

Bassam Burgan¹, Vincent H Y Tam², Mike Johnson², Anqi Chen¹, Dan Allason²

¹ Steel Construction Institute, Silwood Park, Ascot, Berks, SL5 7QN, UK

² DNV GL, Spadeadam Testing and Research Centre, MOD R5, Gilsland, Brampton, Cumbria, CA8 7AU, UK

*Corresponding Author: Email Address: vincent.tam@dnvgl.com

Simple objects such as instrument boxes and oil drums are often found on petro-chemical plant sites. In the event of an accidental vapour cloud explosion (VCE), they serve as reliable indicators of the explosion overpressure at their positions provided there is a good understanding of their behaviour in a VCE.

Such objects were used to great effect in estimating the overpressure magnitude in the Buncefield incident in 2005. In large scale tests conducted since the Buncefield incident (both as part of a joint industry project and subsequently), such objects were located at varying distances from the cloud, as well as some within the cloud. Overpressure measurements were made at or adjacent to the location of these objects and many have been analysed using advanced finite element analysis. The objectives were to (i) gain a better insight into the response of these objects when subjected to different types and magnitudes of pressure loading, (ii) assess the suitability of different finite element modelling techniques for predicting the response of these structures and (iii) develop pressure impulse (PI) diagrams which can be used to provide a rapid assessment of explosion magnitude through an examination of the damage level.

This paper presents an overview of the tests performed and the analysis results with comparisons with the actual behaviour of the objects.

Introduction

The reliability with which the characteristics and severity of a gas or vapour cloud explosion (VCE) can be interpreted is dependent on information on the overpressure distribution and propagation direction. In a controlled experiment, there are sensitive instruments that measure the rapid changes in overpressures with time, flame speed and direction and stresses and strains in objects responding to the explosion loads. These characteristics have to be inferred from observations of damage in the post incident survey. However, the vast majority of objects in a typical refinery or oil and gas facility, e.g. structures and equipment, are complex objects with unpredictable response. This makes diagnosis of VCE characteristics difficult.

During the Buncefield investigation and subsequent research (MIIB 2008, UK HSE 2009, SCI 2014, Atkinson 2009 and Tam 2011), we identified objects located in and around the Buncefield site that could help in the explanation of the explosion mechanism. If the response characteristics of such objects can be fully described, they would form an important tool in the diagnosis of a VCE event.

Common Objects

The majority of objects found in the Buncefield accident are complex. The three types of objects used in the investigation and research projects to interpret the Buncefield explosion mechanism were cars, boxes and drums. For the purpose of this paper, cars are too complex and have been excluded.

The objects we selected are boxes and drums. In this paper, we use electrical/electronic instrument switch boxes and standard 45 gallon steel oil drums. Both physical testing and numerical finite element methods were used. Physical testing involve subjecting these objects to explosion loads.

Physical Testing

Boxes and drums were exposed to a range of loading: (a) shock load originated from detonations, typically, the duration is short (~ a few ms) and (b) a longer duration (~ 10's of ms) loading from deflagration with a similar rise time and decay time before and after the peak. The tests were performed at the Spadeadam Testing and Research Centre.

Detonation tests were carried out in a gas cloud 30 m long, with a range of widths from 4 m to 10 m and height of between 2 and 4 m. Figure 1 shows a typical construction of a detonation rig. The gas cloud was contained by polythene sheet which was supported by a steel frame. Objects were placed inside and outside of the gas cloud. Pressures were measured close to the objects. Figure 2 shows an example of pressure time profile both within the detonated cloud and external to it. It can be seen that both pressure profiles show 'shocked' characteristics. The duration of the external overpressure was much longer, at about 10 ms to 20 ms, than that inside (about 5 ms).



Figure 1: A picture of one of the rigs in which detonation test was carried out.

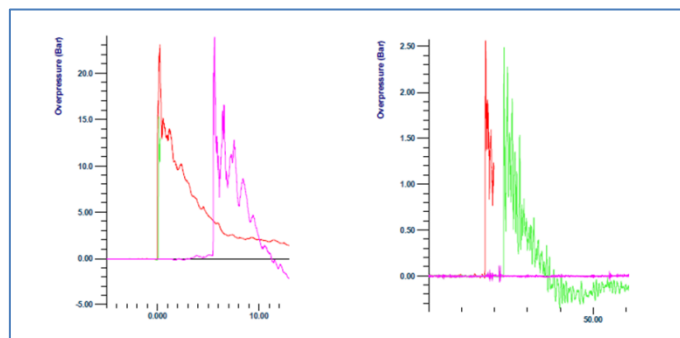


Figure 2: Example of overpressure profiles within the detonated cloud (left) and some distance away (right).

Deflagration tests were carried out using the bang box. The box measures 4.5 m wide, 4.5 m high and 9 m long. This is used routinely for testing the resistance of objects or structural elements such as walls against specified overpressures. The overpressures characteristics are controlled by the choice of gas, the vent area and the amount of congestion inside. Additional deflagration tests were carried out on boxes using the congestion rig at GexCon in Norway. The overpressure range was lower (≤ 2 bar). Figure 3 shows the bang box and a typical overpressure-time profile. In this case the maximum pressure is about 1.4 bar with a duration of about 110 ms.

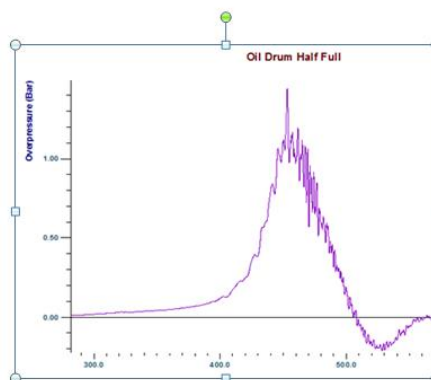


Figure 3: A picture of the bang box and an example of pressure-time profile produced in one of the tests. The vent area of the bang box is shown covered for protection of the internal equipment against the environment.

Results Instrument Box Tests

Standard 150 cm electrical switch boxes were exposed to shocked load from a detonation, being outside the detonating gas cloud. Figure 4 shows the response of the boxes to a range of overpressures and durations. Overpressures from detonations typically have very short duration. As the shock wave propagates away from the cloud, the dispersion effect lengthens the duration. In the example shown in the figure, this was increased to a maximum of 10 ms in the range of distances that the boxes were located. At less than 3 bar, these boxes had no visible permanent deformation. At higher pressures, permanent damage increases as overpressure increases. The damage was predominant on one side. However, the deformation is different from the box that was located within the detonation; the box was squashed on all sides.



Figure 4: Switch boxes exposed to shock loading of a range of pressure and durations. The incident overpressures were (from left to right) 8.2 bar, 3.4 bar, 2.1 bar and 0.7 bar. Duration ranges from 4 ms to 10 ms.

Steel Oil Drums

Standard steel oil drums were located outside a detonation cloud at various distances. Figure 5 shows the final state of the drums after exposure to a range of overpressure between 0.4 bar and just over 4 bar with duration of around 10 ms. For comparison, the drum located within the detonation is also shown. At less than 2 bar, the standard steel oil drum suffered very minor deformation. The drums were 50% filled with water, except the one on the far right of Figure 5 which was two third filled.



Figure 5: Drums exposed to shock loading of a range of pressures and durations. The one on the far right was inside a detonation cloud. For the three on the left and from left to right, the maximum incident overpressures were 4.4 bar, 2 bar, and 0.4 bar and the respective durations were 10 ms, 11 ms and 15 ms.

Steel drums exposed to a range of deflagration overpressures are shown in Figure 6. At 0.7 bar and a duration of 160 ms, the drum did not show any sign of damage. At a pressure of over 1 bar, permanent damage was observed. The two drums shown in Figure 6 were 75% filled with water and exposed to overpressures of 1.4 bar and 1.8 bar with durations of 110 ms and 43 ms. The damage characteristics are different to those by detonation even though the permanent deformation suffered by both sets of drums can be described as “creased”.



Figure 6: An oil drum (left) after it has exposed to a deflagration loading of 1.4 bar and duration of 110 ms (centre) and one exposed to an overpressure of 1.8 bar with a duration of 43 ms (right).

Discussions on physical testing

It can be seen that the damage suffered by both boxes and steel drums varies with peak pressure and duration. This phenomenon is well known. Structural engineers have developed a damage assessment criteria based on two parameters: maximum pressure and impulse (which is the area under the pressure time curve). This is usually presented in a pressure-impulse diagram (PI diagram). In effect, the duration part of the pressure time profile is taken account of in impulse. Work

is in progress to collect more data in order to construct a more complete PI diagram using data. The work to use finite element analysis to calculate the response of the box to VCE loading is presented in sections below.

Like boxes, within a detonation, drums are completely squashed above the liquid level (see Figure 5). Tests show that steel oil drums are more resilient to overpressure loading than switch boxes at short durations of less than 10 ms. A steel drum is a more complex object than a box with many modes of vibration, hence the drum’s response behaviour is also more difficult to characterise. There are more variations in observed damage for different overpressures and durations. In order to uniquely identify the properties of the overpressure wave, more data are needed for the characteristics of damage from further physical testing and FE analysis. The work towards this is in progress.

As can be seen from the figures, explosion loads produce creases on the surface of drums. Apart from the obvious differences in character from those observed in a detonation, there are also differences when similar pressures of different durations are applied. Work on drums at low overpressures (< 2 bar) by Horn et al (2015) showed variation of damage with overpressure and duration. However, there was no pictorial information, and short description of damage does not allow comparison with our data.

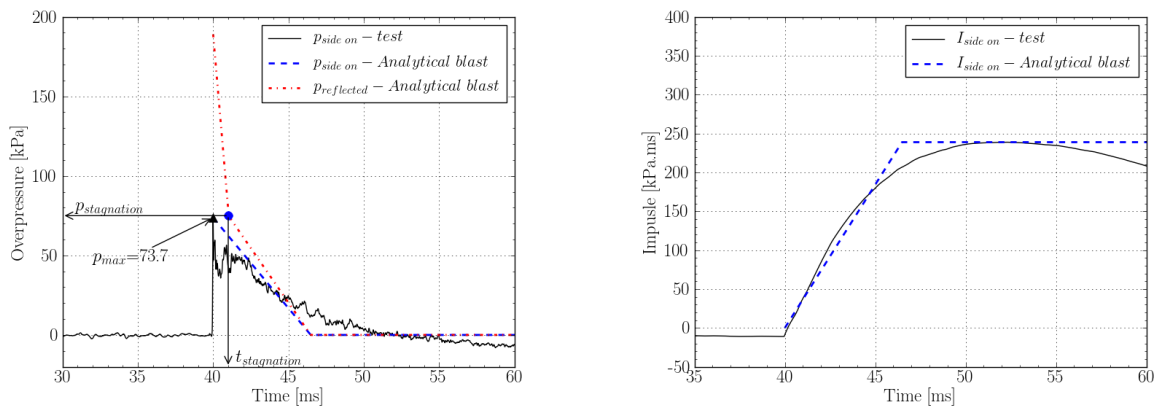
Numerical Analysis

The analysis being reported here is for instrument boxes. A number of different analytical techniques were compared by Chen (2014) to determine the accuracy of the methods when used for this type of problem. These were Lagrangian, uncoupled Eulerian-Lagrangian and coupled Eulerian-Lagrangian analysis (in increasing order of computational demand). The difference between the three approaches is briefly outlined below. Drums are more complex to model than boxes and as they are not fixed in position and their form is sensitive to the way in which the load acts on the drum. The methodology and results described below will be used to guide future work on drums and other simple objects.

Lagrangian analysis

In a Lagrangian analysis, the box is modelled using shell elements and the blast load is applied directly to the surface of the elements as a uniformly distributed load. The reflected and side on blast loads were derived using an analytical method using the blast wave parameters (peak overpressure and impulse) of the incident blast wave from the tests.

The reflected load is applied to the front face of the box (the door). Given the relatively small dimensions of the boxes, there is negligible pressure decay as the blast wave passes over the boxes. Therefore, the other faces of the box are subjected to loading that closely matches the measured side on pressure. A comparison of the overpressure and impulse measured in the test with the derived values for one of the boxes is shown in Figure 7.



(a) Overpressure measured in the test and derived load used in the Lagrangian analysis

(b) Impulse derived from test measurements and derived impulse used in the Lagrangian analysis

Figure 7 Example of loading used in the Lagrangian analysis (shown for a small box at 15 m from the edge of the cloud in Test 4.2-4)

Uncoupled Eulerian-Lagrangian analysis

This is a two-step approach. In the first (Eulerian) step, the box is treated as a rigid object and a high intensity blast wave generated by the expanding gases propagates through air from the origin of the explosion towards the box (Figure 8). The Eulerian analysis produces the dynamic pressure-time traces acting on all the surfaces of the box.

Once calculated, these pressures are then applied to the box in the second (Lagrangian) step of the analysis. Provided the deformation of the box has negligible influence on the development of the pressure loading on the surfaces of the box, this method is expected to give accurate results.

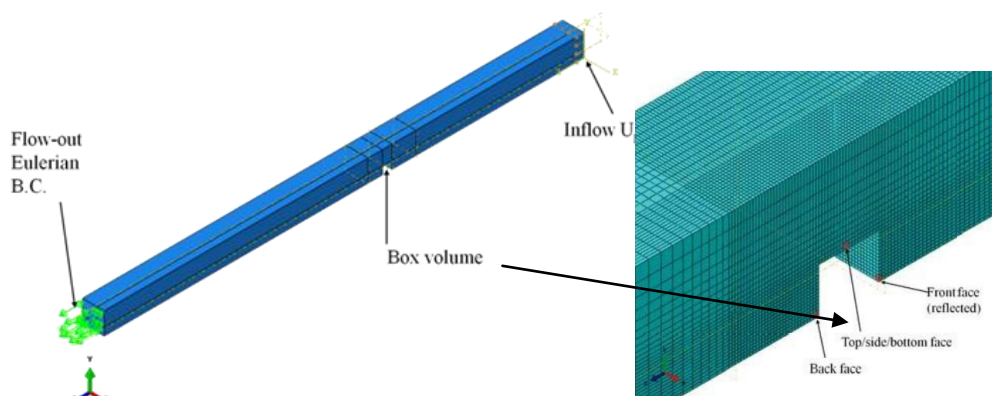


Figure 8 Eulerian model (only ¼ of the model is shown taking account of symmetry)

Coupled Eulerian-Lagrangian analysis

Using this approach, the Eulerian and Lagrangian models are combined (Figure 9). Interaction between the blast wave and structural deformation is accounted for by the model which allows for contact between the Eulerian and Lagrangian parts. This is the most accurate approach where the interaction of the structure of the box influences the way in which the pressure acts on the surfaces of the box. This is likely to be the case where the pressures are relatively high and the box deformations large. The method is, however, computationally very demanding and as such is not suitable for general use.

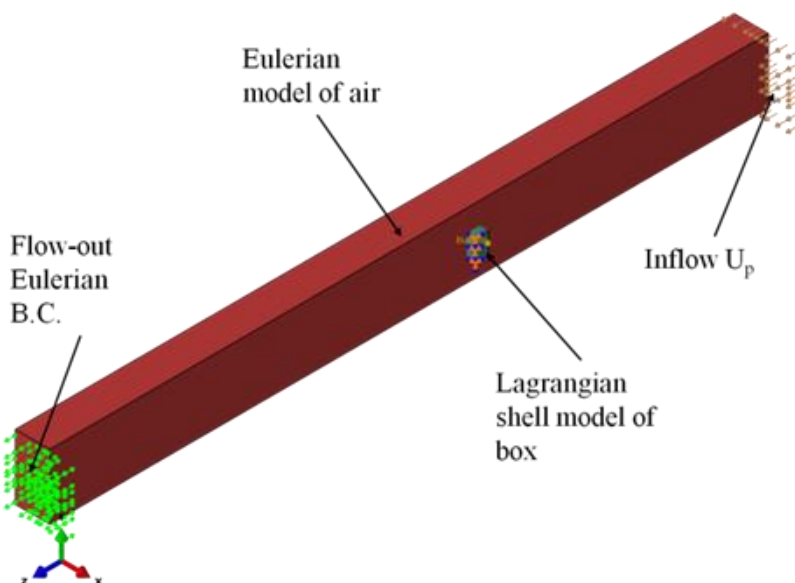


Figure 9 Combined Eulerian-Lagrangian model (only ¼ of the model is shown taking account of symmetry)

The starting point to both the coupled and uncoupled analyses is to calibrate the model so that it represents the free field incident blast wave. This is done using a one-dimensional Eulerian model and imposing a particle (inflow) velocity at the inlet boundary of the model. A trial and error process (including variation of the particle inflow velocity) is used to determine the correct numerical blast wave with the same peak overpressure and impulse as measured in the tests.

The difference in computational demand can be illustrated by comparing the run-time for a typical blast analysis of one of the boxes. The run times on a high performance computer are 2 minutes, 57 minutes and 15 hours for the Lagrangian, uncoupled and coupled analysis respectively.

Instrument box models

The body and door of the boxes were modelled using shell elements. The door hinges and lock were modelled using rotational hinges. A typical model is shown in Figure 10. The box is supported horizontally and vertically along its two back vertical edges and around its base perimeter. The boxes are made of galvanised steel with nominal plate thickness 1.25 mm, average yield stress 279 N/mm² and average ultimate stress of 297 N/mm².

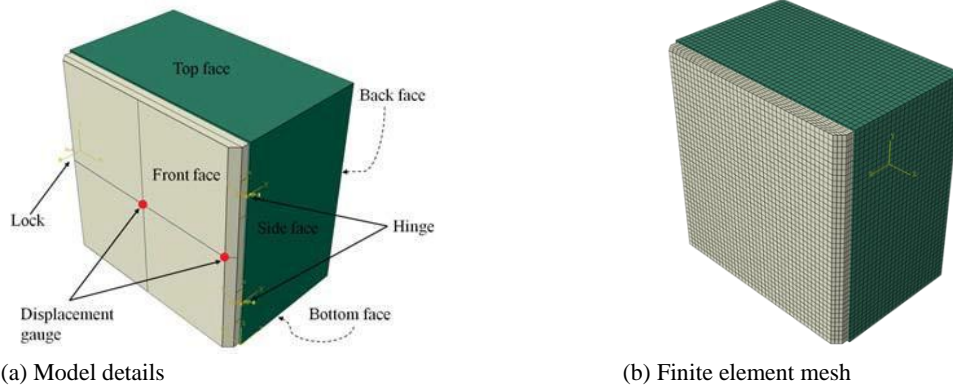
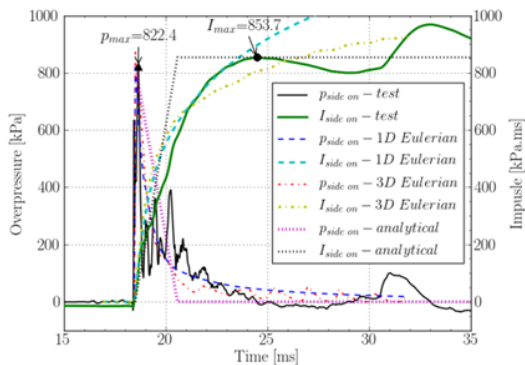


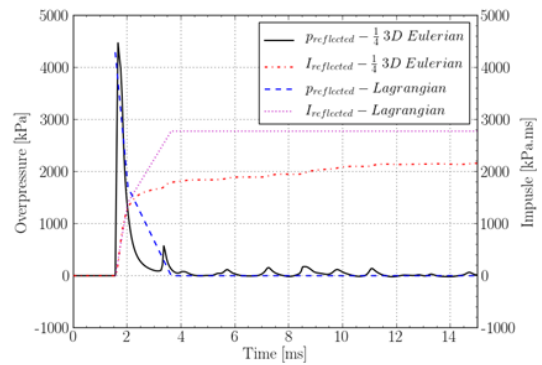
Figure 10 Numerical model for a 300 x 300 x 200 box

Analysis Results

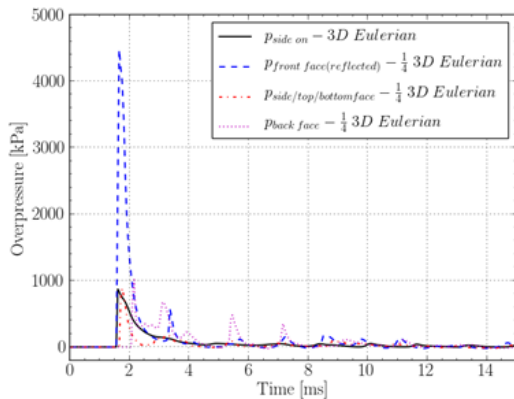
The boxes were analysed using the three analytical methods described above. The methodology is illustrated by reference to the small box in Test 4.2-4 located at a distance of 4 m from the edge of the cloud. The first (calibration) step in both the coupled and uncoupled analyses is illustrated by reference to Figure 11(a). It shows the experimental free field overpressure-time trace (and the corresponding impulse), the calibration free field pressure and impulse (using a 1-D analysis) and the free field pressure and impulse generated by the 3-D Eulerian analysis using the parameters derived from the 1-D calibration. In Figure 11(b) the reflected overpressure time history and impulse derived from the analytical method are compared with those calculated by the Eulerian analysis. Figure 11(c) shows the overpressure time profiles on all box faces calculated in the first step of the uncoupled Eulerian-Lagrangian analysis. These are the loadings sustained by the box in the uncoupled analysis. Figure 11(d) shows the results of the analysis using the displacement at the centre of the door as a reference point. It can be seen that the coupled Eulerian-Lagrangian analysis is in close agreement with the test, while the uncoupled analysis and the Lagrangian analysis overestimate the deflection.



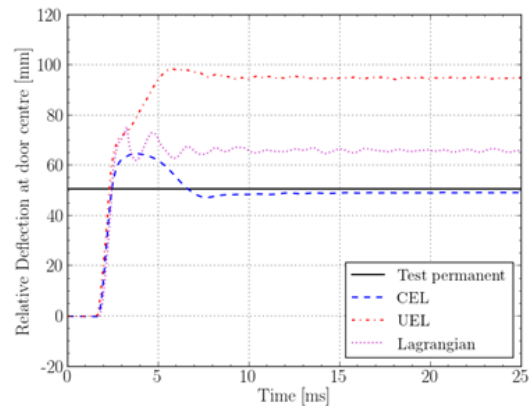
(a) Calibration of inflow velocity and derivation of numerical free field blast wave



(b) Comparison of numerical reflected pressure derived by simplified calculations and using the 3-D Eulerian analysis



(c) Overpressure loading on all the box faces calculated using Eulerian analysis



(d) Box door centre displacement calculated using the three methods compared with the measured permanent deformation in the test

Figure 11 Analysis results for a small box in Test 4.2-4 at 4 m from the cloud edge

The deformed shape of the box as determined by the three analysis methods is compared with the image of the box after the test and with the laser scan record of the box shown in Figure 12.

In the following figures and tables coupled Lagrangian-Eulerian analysis is referred to as “CEL”, uncoupled as “UEL” and pure Lagrangian analysis as “L”.

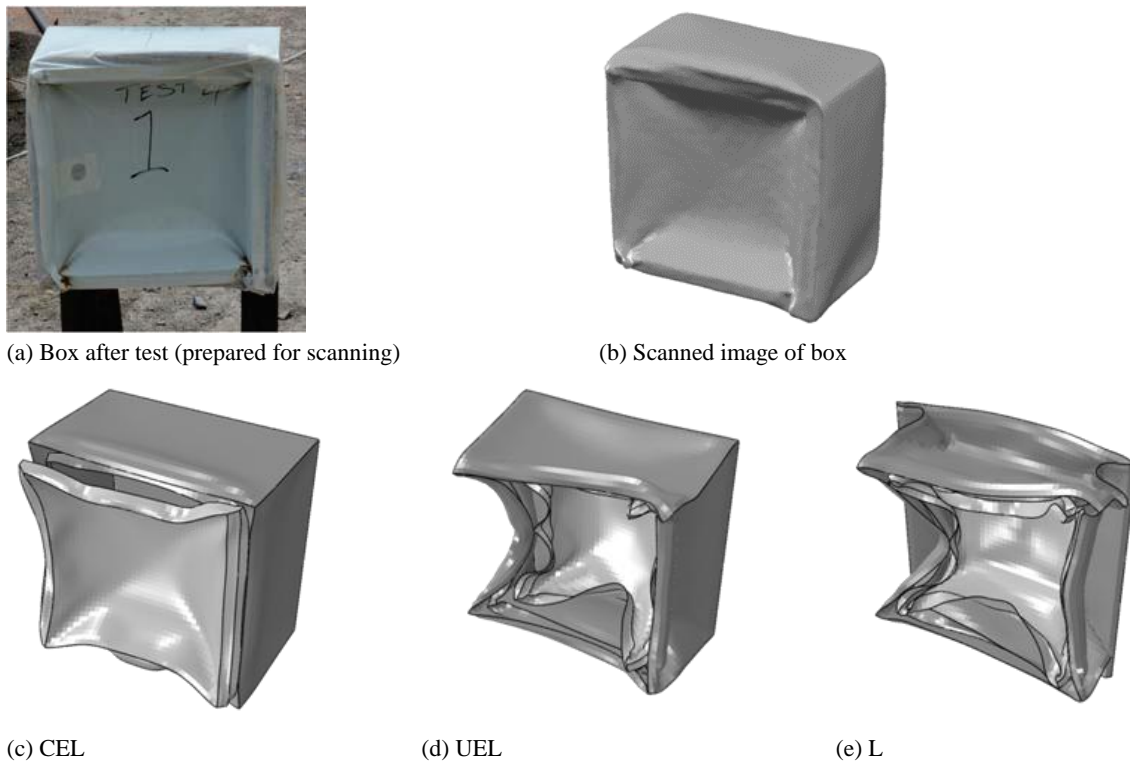


Figure 12 Actual and predicted deformed shapes

A summary of the results for the boxes is shown in Table 1. The numbers below the images are the permanent deformation in mm at the centre of the door of the box. This deflection was measured relative to the middle of the box vertical edge of the box (from the laser scanned record for the tests and from the finite element model in the case of the analyses). This is illustrated in Figure 13 for a scanned image of one of the boxes.

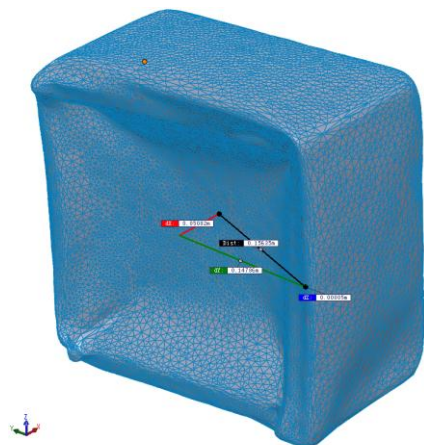


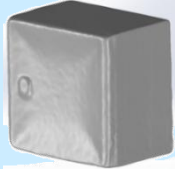
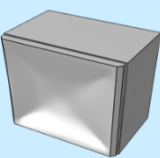
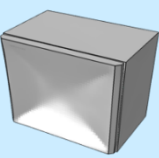
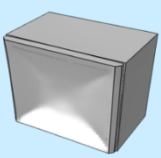
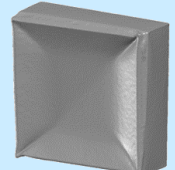
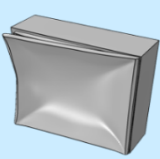
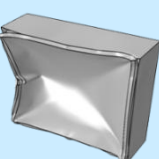
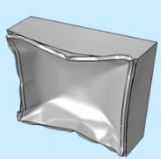
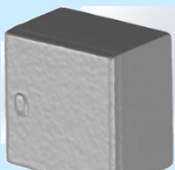
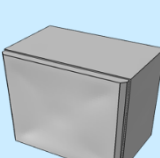
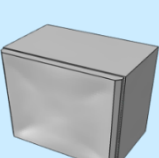
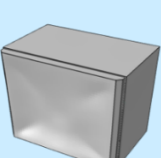
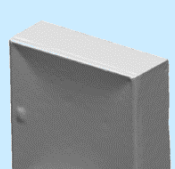
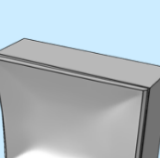
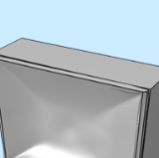

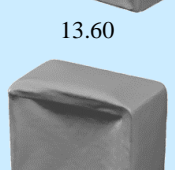

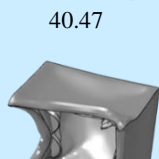


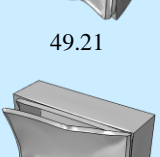

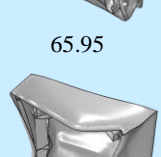
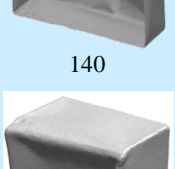
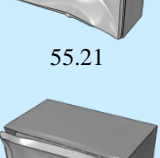
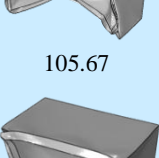
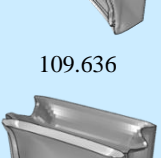
Figure 13 Door centre deformation measurement


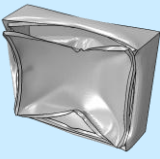
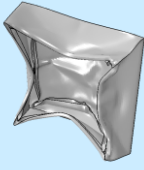
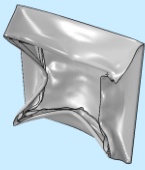

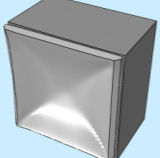
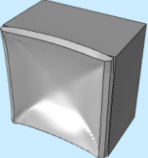
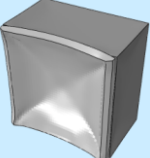
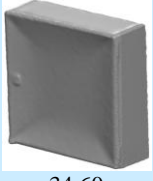
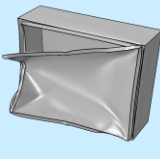
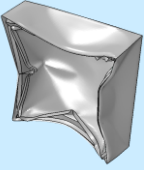
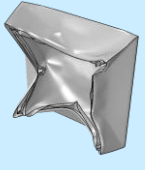

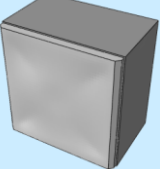
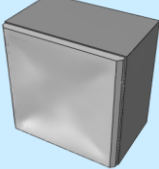
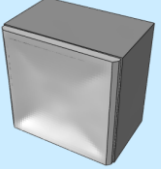

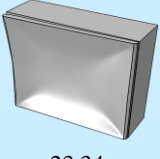
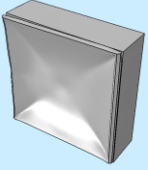
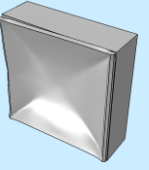
In all but the most severely deformed boxes the side edge remained straight. However, where the side edge deforms, this can give rise to misleading comparisons as illustrated for example in Figure 12(e) and is a particular problem in the Lagrangian analysis where application of the incident pressure to the side wall can cause premature buckling of the wall and hence inward movement of the vertical edge.

As a general observation, very good agreement was found between the CEL analysis and the measured deformation for the small boxes. Pressure transducers were located on the major axis of the rig alongside the small boxes. The large boxes were

located off the major axis and the pressures were estimated. The overpressure values used in the analysis were generally at the upper limit of the estimated range. Consequently, the calculated deformations in the analysis tend to be higher than those measured in the case of the large boxes.

Table 1 Summary of instrument box analysis results

Test	Box	P (mbar)	Permanent deformation at door centre (mm)			
			Laser scanned box	CEL	UEL	L
4.2-2	Small 15 m	1126	 11.67	 10.53	 13.85	 15.00
	Large 15 m	1126	 59.45	 45.21	 95.32	 98.89
4.2-3	Small 15 m	693	 0.26	 0.53	 4.21	 5.87
	Large 15 m	693	 13.60	 24.92	 40.47	 38.84
4.2-4	Small 4 m	8224	 50.59	 49.21	 94.89	 65.95
	Large 4 m	4345	 140	 55.21	 105.67	 109.636
	Small 6 m	3428	 32.6	 42.4	 55.4	 54.5

Test	Box	P (mbar)	Permanent deformation at door centre (mm)			
			Laser scanned box	CEL	UEL	L
Large 6 m	3428					
		68.00	100.97	85.18	65.71	
Small 10 m	2067					
		9.91	24.28	32.09	35.48	
Large 10 m	2067					
		34.60	54.27	130.68	83.71	
Small 15 m	737					
		1.55	1.62	4.62	6.83	
Large 15 m	737					
		-2.00	23.34	34.59	41.19	

Pressure-Impulse and Explosion Damage Diagrams

Pressure-impulse diagrams have been constructed for the small instrument boxes using the validated finite element model. A range of the free field incident overpressure of 10 to 400 kPa (100 mbar to 4000 mbar) corresponding to a reflected overpressure range of 20 – 1665 kPa (200 mbar to 16650 mbar) was used. The impulse range covered was from 10 to 10000 kPa.ms (100 mbar.ms to 100000 mbar.ms). The resulting P-I diagram is shown in Figure 14 for door centre deformations ranging from 1 mm to 40 mm.

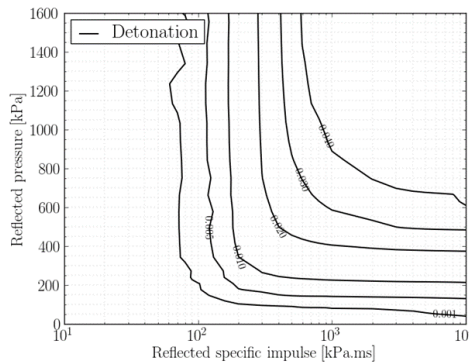


Figure 14 P-I diagram for 300 × 300 × 200 boxes subjected to a detonation

It should be noted in the above that box sidewall buckling may occur when the incident pressure is greater than 200 kPa (2000 mbar) corresponding to a reflected overpressure of 660 kPa (6600 mbar). When this happens, the relative deformation of the centre of the door to the edge remains in the range of 50 – 60 mm as the whole door moves back into the box.

Summary

The detailed response of an object exposed to a VCE loading depends on the properties of the pressure loading, such as peak overpressure, duration and load-time profile. Given a good knowledge of the damage suffered, it is possible to use objects as diagnostic tools in incident investigations to provide accurate information to characterise VCEs involved. Steel drums and switch boxes are simple objects commonly found in petrochemical and oil and gas facilities.

Damage to two groups of simple objects, steel drums and boxes had been characterised using physical testing. Finite element analysis has also been carried out for steel boxes. Based on the FE analysis, a pressure-impulse diagram incorporating iso-deformation or iso-damage curves were produced. The same principle can be applied to boxes of different sizes and aspect ratios, and to other objects.

More complex objects than a simple box exhibit more complex response behaviour, producing a range of damage pattern. Hence it is important to include pictorial information.

This paper shows that the principle of using simple objects as an indicator of the characteristics of VCEs, further work is needed to (a) gather data from physical tests, and (b) further develop FE models for more complex object than boxes. This research is ongoing.

References

- Atkinson, G.A., Cusco, L. and Tam, V.H.Y., Interpretation of overpressure marker and directional indicators in full scale deflagrations and detonations, Hazards XXI conference, Manchester, UK, Nov, 2009.
- Chen, A., Structural Response to Vapour Cloud Explosions, PhD Thesis, Imperial College, London, 2014.
- Horn, B.J., Goodrich, M.L. and Thomas, J.K., Deflagration load generator: repeatability and application to test article blast loading. 11th Global Congress on Process Safety, Texas, U.S.A., 27-29 April 2015.
- Kinnley G. F. and Graham K.J., Explosive shocks in air, Springer Verlag, 1985.
- Major Incident Investigation Board, The Buncefield Incidence 11 Dec 2005 Vol 1 and 2, ISBN 978 0 7176 6270 8
- Burgan, B. A., Dispersion & Explosion characteristics of large vapour clouds, The Steel Construction Institute, 2014 (available at <http://www.fabig.com/video-publications/OtherPublications>).
- Tam, V.H.Y., The Buncefield accident, why was the explosion so severe? Loss Prevention Bulletin 222, published by the Inst. Chemical Engineers, December 2011.
- UK Health and Safety Executive, Buncefield Explosion Mechanism Phase 1, volume 1 and 2, HSE Research Report, RR718, dated 2009